applied sciences

MDPI

Article

Geomechanical Characterization of a Brazilian Experimental Site: Testing, Interpretation, and Material Properties

Jair de Jesús Arrieta Baldovino [1,2,*], Yamid E. Nuñez de la Rosa [2] and Marcos Massao Futai [3]

[1] Civil Engineering Program, Universidad de Cartagena, Cartagena de Indias 130015, Colombia
[2] Faculty of Engineering and Basic Sciences, Fundación Universitaria Los Libertadores, Bogota 110231, Colombia; yenunezd@libertadores.edu.co
[3] Department of Structural and Geotechnical Engineering, Polytechnic School, University of São Paulo, Ave. Prof. Luciano Gualberto, 380, Cidade Universitária, Butantã 05508-010, SP, Brazil; futai@usp.br
* Correspondence: jarrietab2@unicartagena.edu.co; Tel.: +57-304-260-2846

Abstract: Clarity in monitoring existing foundation structures demands innovative safety analysis methodologies for deep foundations, necessitating advanced models calibrated with real-world field parameters. Understanding controlled conditions, including geotechnical profiles, seismic attributes, and soil mechanics, is crucial. A dedicated research group at the University of São Paulo spent three years refining these conditions, characterizing an experimental field along a canal in São Paulo. This study pioneers geotechnical and geomechanical characterization of the region's tertiary sediments in São Paulo, offering valuable insights for current and future applications. Standard penetration tests with torque (SPT-Torque), piezocone tests (CPTu), and measurement of wave velocity (Vs) with piezocone tests (S-CPTu) were carried out. The exploration of the subsoil shows that in up to 2 m of excavation, there are clays and silts, and in up to 25 m, there is a significant layer of compact fine sand that has high values of tip resistance and wave velocities more significant than 100 m/s. In the electric cone tests, the abacus used displayed a reasonable classification. All propositions identified the transition from the surface soil to the sandy soil at between 3 and 25 m. The soil classification values were obtained with the data of the field parameters, and the geotechnical and mechanical parameters were estimated. No differences were detected among the values found in the SPT-T and CPTu tests for the values obtained via cone resistance. This demonstrates the reliability of both methods. In addition, using the CPTu test to identify the stratigraphic profile horizons employing the soil's mechanical behavior when the cone is driven proved appropriate.

Keywords: experimental site; geotechnical characteristics; piezoelectric cone; seismic velocity

check for updates

Citation: Arrieta Baldovino, J.d.J.; Nuñez de la Rosa, Y.E.; Massao Futai, M. Geomechanical Characterization of a Brazilian Experimental Site: Testing, Interpretation, and Material Properties. *Appl. Sci.* **2024**, *14*, 5656. https://doi.org/10.3390/app14135656

Academic Editor: Jianhong Ye

Received: 21 May 2024
Revised: 20 June 2024
Accepted: 23 June 2024
Published: 28 June 2024

Copyright: © 2024 by the authors. Licensee MDPI, Basel, Switzerland. This article is an open access article distributed under the terms and conditions of the Creative Commons Attribution (CC BY) license (https://creativecommons.org/licenses/by/4.0/).

1. Introduction

Given the escalating demand for precise monitoring of existing foundation structures, it becomes imperative to pioneer novel methodologies for the safety analysis of deep foundations. This necessitates advancing and calibrating stability and load capacity prediction models using real-world field parameters. Consequently, a comprehensive understanding of controlled conditions, encompassing the intricate interplay of geotechnical profiles, seismic attributes, and soil mechanics properties, emerges as paramount. Undertaking meticulous calibration tests in experimental fields assumes critical significance as these serve as crucial benchmarks for subsequent applications in real-world scenarios involving the studied foundations. Over three years, a dedicated research group at the University of São Paulo (Southern Brazil) has fervently devoted its endeavors to meticulously establishing and refining the conditions above. Subsequently, an experimental site within the university premises was meticulously selected for intensive investigation. This study presents a rigorous geotechnical and geomechanical characterization of the experimental field nestled along the banks of a small canal. Situated within the Planalto Paulistano,

amidst the tertiary sediments of the São Paulo Basin, the city of São Paulo provides a fitting backdrop for this pioneering endeavor.

Within the university campus itself (named POLI/USP-EPUSP/LMS), more than 3 km away, an experimental field was installed in 1988. The experimental field was created through a joint action between the Polytechnic School and ABEF—Brazilian Association of Foundations and Geotechnical Engineering Companies, aiming to conduct research involving the performance of some types of foundations. The primary motivation was to prepare a special report reflecting national competence in this area when the XII International Congress of Soil Mechanics and Foundation Engineering was held in Rio de Janeiro in 1989. With the support of 22 companies running foundations and four technology institutions, the research was presented at that event in a particular publication, with 86 pages covering the main results. In recent years, buildings for academic purposes have been built within the premises. The conditions, location, geological-geotechnical characterization, and mechanical properties of the experimental field are explained in detail in the study of Cavalcante et al. [1].

The current experimental fields in Brazil are located in six Brazilian states in the South (State of Paraná), with three fields, Southeast (São Paulo and Rio de Janeiro), with six fields, and Central-West (Distrito Federal) and Northeast (Pernambuco), with one field each. Other experimental fields in Brazil have made excellent contributions to geotechnical engineering, such as UFRGS, UFBA, and SENAC-SESC (Rio de Janeiro). Still, new fields are needed to better understand soil behavior in Brazil. The oldest experimental field in Brazil is the COPPE/UFRJ-PUC-Rio (IPR-DNER)/Sarapuí field, created in 1974 with a study area of 42,000 m^2. However, the largest field was created in 1991 by UNESP/FEB with a total area of 50,000 m^2. Recently, the most studied fields are the experimental field of Araquari and the UPF/UFRGS in the country's south.

Field tests currently form the basis of developing an essential number of engineering projects. The main advantages of this type of investigation lie in the speed of test execution, the definition of the geotechnical profile, and the possibility of evaluating geotechnical properties under natural field conditions [2]. Through field test results, it is possible to determine, for example, the geotechnical profile of the site, pore pressure distribution, and strength and deformability characteristics. The cone penetration test characterizes fine soil deposits because it evaluates strength and pore pressures within the material. Additionally, if a sensor is attached to the equipment, seismic measurements can be obtained during the same penetration [3].

One of the widely used field tests for assessing soil behavior is the piezocone test since it allows at least three measurements to be obtained in the same penetration: tip resistance (q_c), pore pressures ($u2$), and sleeve friction (q_s). Furthermore, if specific sensors are attached, it is possible to determine shear wave velocity measurements within the soil mass [4]. In soft clays and silts and in overwater work, the measured q_c must be corrected for pore water pressures acting on the cone geometry, thus obtaining the corrected cone resistance, q_t, as defined by Equation (1):

$$q_t = q_c + u2(1 - a) \quad (1)$$

where 'a' is the net area ratio determined from laboratory calibration with a typical value between 0.70 and 0.85. In sandy soils, $q_c = q_t$. Considering the attractiveness of the CPTu test, the interpretation methodologies adopted in this research will be restricted to results obtained from the piezocone test with seismic readings (S-CPTu). The cone penetration test does not allow for sample collection; therefore, material identification is carried out through empirical correlations between the measurements provided by the test. Currently, the most widely used proposals consider the combination of normalized parameters proposed by Robertson [5]. In the case of conducting piezocone tests with shear wave velocity (Vs) readings, Robertson et al. [6] proposed a graphical methodology for soil characterization and behavior evaluation based on normalized cone resistance (Q_{tn}) and the ratio between the maximum shear modulus and the cone tip resistance (G_o/q_t). Also, using the combination

of resistance and stiffness parameters, Eslaamizaad and Robertson [7] utilized the G_o/q_c (where q_c is the tip resistance of cone) versus q_{c1} space to characterize cementation and compressibility properties of granular soils, where q_{c1} is defined according to Equation (2). Since cone penetration in granular soils occurs under drained conditions, the proposal utilizes cone tip resistance (q_c) values without corrections for pore pressure effects.

$$q_{c1} = \left(\frac{q_c}{p_a}\right)\sqrt{\frac{p_a}{\sigma'_{vo}}} \quad (2)$$

where p_a is the atmospheric pressure and σ'_{vo} is the effective vertical stress acting at the depth of the test measurements. Recently, Schnaid et al. [8] used the identical G_o/q_c versus q_{c1} space to introduce boundaries for cemented and non-cemented sands obtained through tests conducted in calibration chambers. These boundaries indicate the classification of granular soils, composing diagonal contours that delineate the upper and lower limits for sands without aging and cementation and the upper and lower limits for sands with aging or cementation.

Recent advancements in geotechnical investigations facilitated by Cone Penetration Testing (CPTu) have witnessed significant progress through groundbreaking studies. One noteworthy development involves the application of Bayesian Mixture Analysis to a comprehensive global database [9], resulting in a substantial improvement in the prediction accuracy of unit weight. Moreover, the field has seen the emergence of a sophisticated probabilistic Bayesian methodology designed to correct the strain rate associated with dynamic CPTu data [10]. This innovation not only refines the precision of measurements but also broadens the scope of dynamic CPTu applications. A straightforward yet powerful probabilistic approach has been introduced for generating geotechnical stratigraphic profiles using CPTu data [11]. This method simplifies the process, making it more accessible while retaining a robust probabilistic foundation. Another pivotal contribution comes from hydromechanical modeling, with Boschi et al. [12] presenting a coupled approach that sheds light on cone penetration dynamics in layered liquefiable soils. The insights derived from such modeling hold significant implications for understanding soil behavior in complex geological settings.

Statistical assessments have also played a crucial role in recent research endeavors, exemplified by Zhang et al. [13], which focuses on simplifying CPTu-based hydraulic conductivity curves. This statistical perspective enhances our ability to interpret and utilize CPTu data effectively. Similarly, the utility of CPTu in assessing changes in shear modulus G_o within the subsoil has been underscored [14], emphasizing its practical relevance in geotechnical applications. Further expanding the horizons of CPTu applications, Liu et al. [15] proposed a method for predicting soil thermal conductivity through Thermal Piezocone Penetration Testing (T-CPTu). This innovative approach aligns with the importance of understanding thermal characteristics in geotechnical analyses. Chmielewska [16] also delves into evaluating compressibility in organic soils, considering both in-situ and laboratory tests, particularly for road construction applications. Geographical relevance is demonstrated in Zhang et al. [16], which explores the geotechnical characteristics of floodplain soils in Nanjing, China, using Seismic Cone Penetration test (S-CPTu) data. This study provides valuable insights into local soil behavior and contributes to the broader understanding of regional geotechnical variations. Finally, Monforte [17] establishes a meaningful correlation between undrained CPTu results and the state parameter for liquefiable soils, enriching our comprehension of soil liquefaction mechanisms. These pioneering studies underscore the depth and breadth of ongoing research in the CPTu field, offering invaluable perspectives that enhance our ability to comprehend and characterize diverse geotechnical subsurface conditions.

The integration of Standard Penetration Test (SPT) results with other geotechnical testing methods has been extensively explored in various studies, highlighting the importance of multi-faceted approaches in soil characterization and engineering projects. Nandi et al. [18] examined the correlation between Pressuremeter Test (PMT) results and

SPT N values for cohesive soils in Kolkata, India. Their study emphasized the value of using PMT alongside SPT to predict soil parameters more accurately, suggesting that PMT can provide reliable additional data for sub-soil characterization. Similarly, San Roman and Botero [19] proposed using Principal Component Analysis (PCA) to integrate data from SPT, Cone Penetration Tests (CPT), and Suspension PS Logging tests. This method effectively identified geotechnical units, improving the accuracy of soil stratigraphy in construction projects. In another study, Sharma et al. [20] focused on correlating geotechnical and geoelectrical properties of soil deposits in India. They found a strong linear correlation between soil resistivity and SPT N values at specific sites, suggesting that geophysical methods complement traditional geotechnical tests to enhance subsurface exploration. This aligns with findings by Puttiwongrak [21], who studied the correlation between electrical resistivity and SPT N-values in the sandy soils of Phuket, Thailand. The authors highlighted the significant impact of geological and climatic factors on the correlation model, demonstrating that regional characteristics must be considered when interpreting resistivity data. Hegde and Anand [22] further investigated the relationship between resistivity and SPT N-values in Patna, India. Their results showed a strong linear correlation, supporting the use of electrical resistivity tests (ERTs) to determine soil design parameters quickly. This approach can significantly reduce the time and effort required for conventional soil testing. Bol [23] proposed a new model based on the soil behavior type index (I_c) to convert CPT data to SPT N values. His model accounted for varying coefficients for different I_c intervals, resulting in more accurate predictions than previous models. Finally, Rocha et al. [24] assessed the applicability of existing correlations for estimating the maximum shear modulus (G_o) from SPT N values in Brazilian tropical soils. They found that classical correlations underestimated G_o for tropical soils, particularly saprolitic ones, indicating the need for region-specific adjustments in geotechnical models. These studies underscore the importance of integrating SPT with other testing methods and considering regional soil characteristics to enhance the reliability and applicability of geotechnical investigations. This multi-method approach provides a comprehensive understanding of soil properties, crucial for the safe and efficient design of foundation structures.

Contributing to understanding of mechanisms that control the behavior of the pile-soil interaction in large-diameter piles executed in sandy profiles was the primary motivation behind proposing the creation of an experimental field. This field was designed to carry out a program for instrumented pile load tests. Some of these studies in the experimental field were published recently by Gamino et al. [25]. This process began with the development of this research, which describes the geotechnical characterization of the study area. The primary goal of this article is to advance geotechnical engineering methodologies to characterize granular soil deposits in Brazil. Another motivation behind this research stems from the critical need to enhance clarity in monitoring existing foundation structures. The objective aligns with the broader context of recent research trends, including Bayesian analysis, probabilistic methodologies, and innovative testing techniques like seismic Piezocone Penetration Testing (S-CPTu). Leveraging insights from these studies contribute to methodological innovation, which is critical for understanding foundation safety analysis. The subsoil exploration and extraction of valuable parameters aim to provide practical applications and insights for current and future endeavors in complex geotechnical settings.

2. Experimental Program

The experimental program was divided into four stages. The first stage consisted of subsoil recognition tests using standard penetration and torque. The second stage consisted of carrying out the piezocone tests, the third seismic tests, and the last stage of extracting samples from the most significant stratum of the geotechnical profile (sandy) for physical-chemical analysis. The experimental program is summarized in Figure 1.

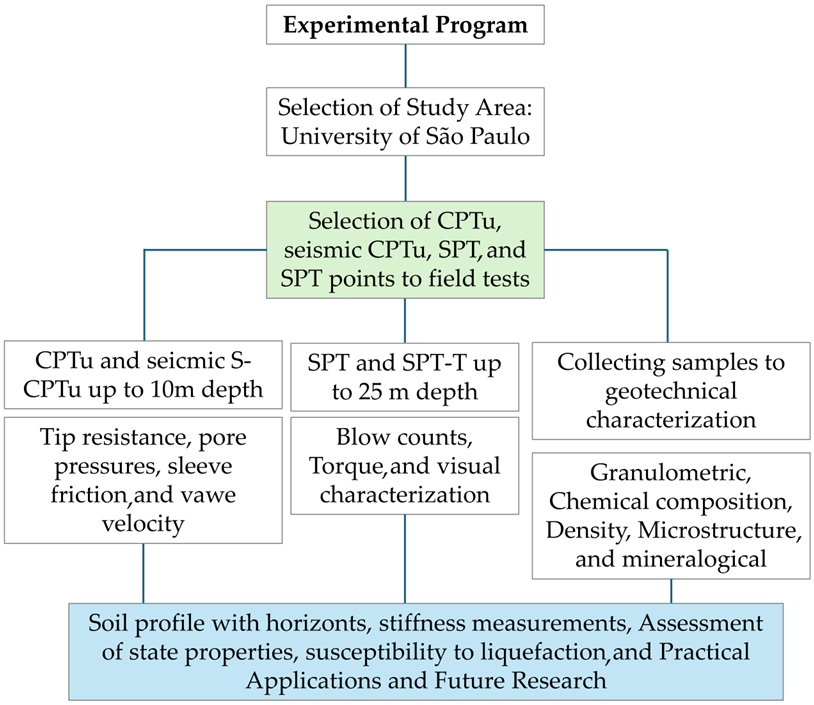

Figure 1. Experimental Program Flowchart.

2.1. General Characteristics of the Study Area

Figure 2 presents the experimental site location. The experimental area is located in the University of São Paulo, Polytechnic School (23°33′13.7″ S 46°43′51.6″ W) in Southern Brazil. The study area is located along a canal approximately 200 m long. The site was chosen because it is a center for full-scale experiments, including recent studies. For example, Gamino et al. [26] studied the soil-structure interaction of pedestrian bridges constructed on this site. Cardoso et al. [27] and Pessin et al. [28] studied the thermal response of energy piles at this site (named CICS Living Lab—see Figure 3). In these studies, the groundwater table depth at the test site varies seasonally from 2 to 4 m.



Figure 2. Map of São Paulo State in Brazil with the location of the cities and the location of experimental site.

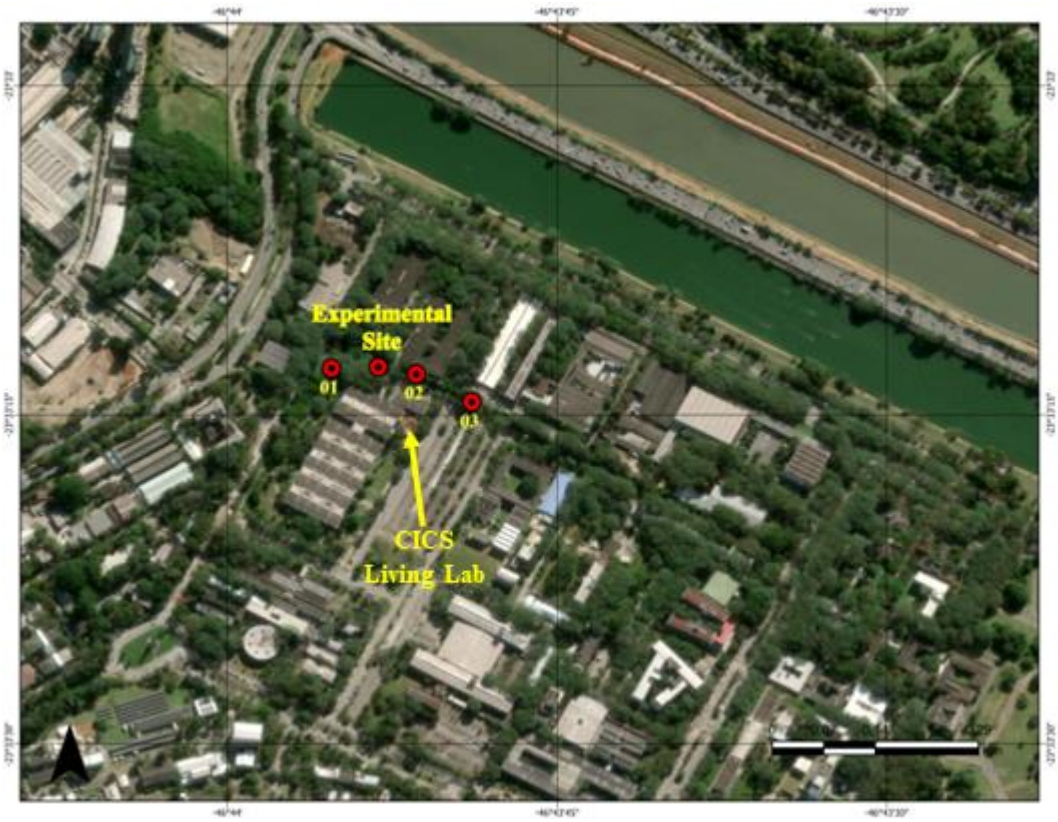

Figure 3. Location of experimental site and characteristics: experimental points 01, 02, and 03.

2.2. Cone Penetration Tests (CPT-u)

The cone penetration test is standardized by American ASTM D-5778-95 and Brazilian NBR 12069/91. The tests involve the penetration of a steel cone, forced statically into the ground, at a constant penetration speed of 2 cm/s, with simultaneous readings of the following measurements: tip resistance q_c, lateral friction resistance q_s, neutral overpressure $u2$, cone inclination, and crimping speed. Measurements are obtained using CPTu equipment with a crimping capacity of up to 20 tf. To read neutral pressures, previously porous stone is used. The saturated stone is located at the base of the cone (reading $u2$). Such saturation is carried out before the test in a vacuum chamber, ensuring total deaeration of the element. Table 1 provides the piezocone experimental program (CPTu), the point's location, the test's depth, seismic depth, and dissipation (with time record).

Table 1. Piezocone experimental program: location of point, depth of test, seismic depth, and dissipation.

Test	Location (North)	Location (East)	Final Depth (m)	Seismic Test (m)	Dissipation (m)	Dissipation Time (min)
CPTu-01	7.394.136,685	323.212,532	7.49	7.50	2.32 3.31 5.01 7.49	29 60 12 9
CPTu-02	7.394.112,691	323.301,811	8.25	7.00	2.30 5.00 8.18	35 9 15
CPTu-03	7.394.075,775	323.436,296	10.17	10.00	3.35 4.76 5.24 10.17	20 11 112 8

The pore pressure dissipation test allows the excess pore pressure induced by penetration (Δu) to dissipate over time. In clean sands, it will dissipate immediately, while in finer materials such as clays, more time will be required for the induced pore pressure to dissipate until it reaches a point (Δu′), which is the hydrostatic pressure.

When penetration is stopped, the time it takes for the induced pore pressure to decrease can be measured. In clays, where the time for this to occur can be very long, it calculates the coefficient of consolidation and hydraulic conductivity. Specifically, these calculations often utilize the time when the induced pore pressure reduces to 50%. Figure 3 presents the location of experimental field points for standard penetration and piezocone tests. The link between points 01 and 03 lies in the nearby structures of interest. For example, in location 01 piles will be built in the future for static and dynamic load testing; in location 02 there is a pedestrian bridge that is being monitored; and in location 03 there is a heavy road load bridge that is being monitored as well.

2.3. Seismic-Piezocone Test (S-CPTu)

The seismic test to measure wave velocity (Vs) is carried out with piezocone equipment according to the procedures of the American standard ASTM D6635-01 [29], and the European standard EUROCODE 7 [30]. In this test, the piezocone is introduced into the ground with a set of rods in a static way. To obtain the wave propagation speed Vs, readings are taken every 50 cm with two geophones coupled to the equipment. A hammer coupled to a drill is used as the source of the shear wave.

2.4. Standard Penetration Test SPT and SPT-Torque

The perforations were made in accordance with the Brazilian ABNT-NBR-6484/20 [31] standard. The descriptions of the collected samples followed the standard established by the NBR6484. Percussion reconnaissance surveys are considered essential by the ABNT foundation standard NBR 6122/19 [32]. However, complementary geotechnical tests may be convenient in certain situations. The sampler used has an external diameter of 50.0 mm and an internal diameter of 34.9 mm. Table 2 presents the Standard Penetration Test (SPT) and SPT-Torque experimental program. In addition, the site contained a characterization of the stratigraphic profile, which was conducted through visual description performed in the field for each extracted sample, identifying changes in the wash mud and its color. The SPT-T tests 01 to 03 were conducted at point 01 marked in Figure 3 (named SPT-01). The SPT-T tests 04 and 05 were conducted at point 02 (named SPT-02), and the SPT-T tests 04 and 05 were carried out at point 03 (named SP-03). This nomenclature has been considered due to the closeness between each test, so the values obtained, which are similar, are averaged.

Table 2. Standard Penetration Test (SPT) and SPT-Torque experimental program.

Test	Location (North)	Location (East)	Final Depth (m)
SPT-T 01	7.394.145,829	323.293,126	25.45
SPT-T 02	7.394.124,216	323.299,672	25.45
SPT-T 03	7.394.074,456	323.438,929	27.45
SPT-T 04	7.394.059,850	323.430,174	25.39
SPT-T 05	7.394.131,402	323.209,687	25.45
SPT-T 06	7.394.133,557	323.223,052	25.45
SPT-T 07	7.394.135,646	323.231,176	25.45

3. Results and Discussion

This section describes the piezocone, SPT-Torque, and soil classification in concordance with field parameters obtained through these techniques.

3.1. Piezocone Test Results and Soil Classification

Figure 4 presents the results of the piezocone tests at points 01, 02, and 03 (Figure 3). For tests CPTu-01, CPTu-02, and CPTu-03, the corrected cone tip resistance (q_c), the sleeve friction resistance (q_s), the measured pore water pressure ($u2$), and the hydrostatic pressure are presented ($u0$).

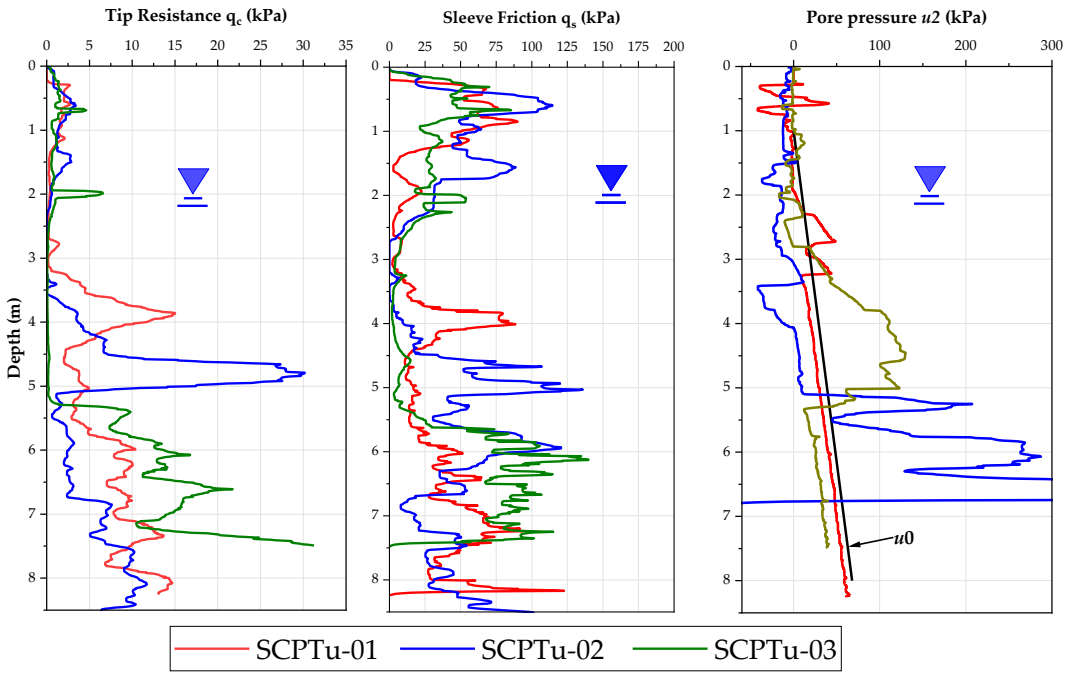

Figure 4. Typical soil profile from piezocone (CPTu) at points 01, 02, and 03 at 20 mm/s penetration.

One of the applications of the CPTu test is to classify soil types based on their behavior and thus obtain a profile of the entire soil. This is based on measurements taken in the field. However, it cannot be expected that the piezocone will provide exact predictions of soil type based on physical characteristics such as grain size distribution. Instead, it guides soil's mechanical characterization (strength, stiffness) [33]. The soil characterization through this test is known as "Soil Behavior Type" (SBT). The normalized cone resistance (Q_{tn}) is the cone resistance expressed in a non-dimensional form, considering the in-situ vertical stresses for SBT characterization. The Q_{tn} is defined as (Equation (3)):

$$Q_{tn} = (q_t - \sigma_{vo})/\sigma'_{vo} \quad (3)$$

where σ'_{vo} is the effective stress and σ_{vo} is the total stress of soil.

Figure 5 was divided into four regions, corresponding to the grain size classification of the soil profile from 0–3 m, 3–6 m, over 6 m, and the complete classification. To better understand the classification and parameters of the soils in the area, the results of the CPTu soundings were superimposed, varying by depth, as seen in Figure 5. These thicknesses were selected considering similar values in cone tip resistance and lateral resistance with depth. This methodology has already been applied in other studies by Schnaid and Yu [34]. From 0 m to 3 m depth, it can be observed that CPTu-02 and CPTu-03 exhibit a similar classification, ranging from very stiff sand to clayey sand. CPTu-01, in the first 3 m, behaves more like normally consolidated soil. From 3 m to 6 m, all three CPTu soundings show that the soil begins to behave similarly, ranging from silty sand to sandy silts. In this layer, the soils exhibit an OCR close to 1, which can be verified in the soil profile after 6 m, where the behavior is close to 1, and the soil classification is sands. Within the geotechnical profile in the first 10 m, no fine sensitive soils were found, nor were many varieties of soils with high stiffness. The data dispersion demonstrates the variability of the stratum along

the studied profile. However, it can be observed that most points are concentrated at the boundary between zones 4, 5, and 6, with some occurrences in zones 7 and 3. In general, the soils found exhibit behaviors typical of non-cohesive soils, such as clean sand to silty sand in zone 6; sandy silts to silty sands in zone 5; and silty clays to clayey silts, normally consolidated, without cementation or aging in zone 4.

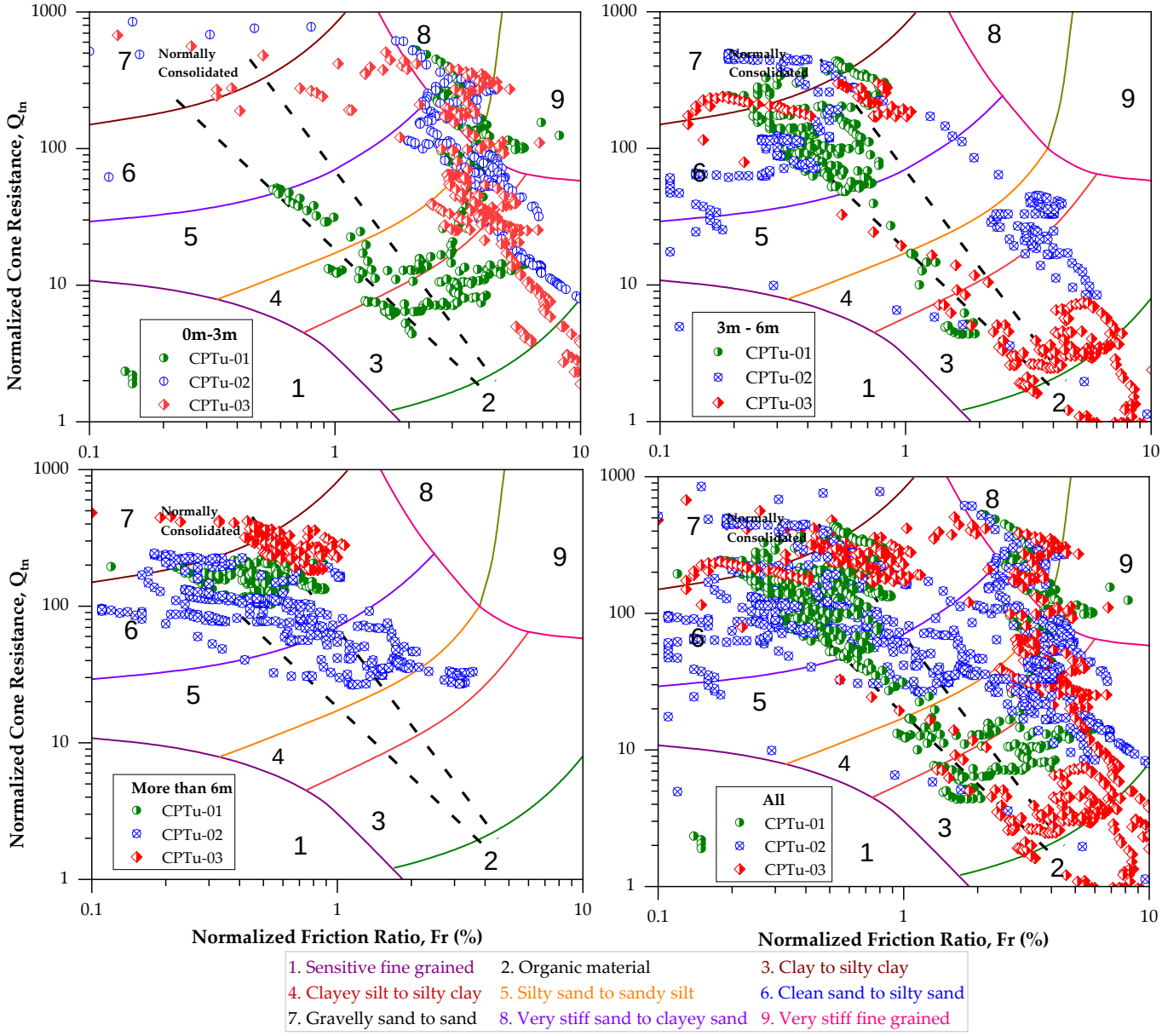

Figure 5. Soil classification, according to Robertson [35].

Figure 6 illustrates the results of G_o stiffness using the methodology proposed by Robertson et al. [6,35], in which parameters of resistance and stiffness are correlated. Although it is recognized that the combination of these two properties serves as a good indicator of soil behavior, the studied soil profile appears to be well characterized in the presented space, predominantly covering a region of clays with low void ratios and regions corresponding to soils with aging and cementation. Figure 6 also compares the G_o measured with accelerometers and G_o estimated with Robertson's [6] empirical relationship for SCPTu-01, SCPTu-03, and SCPTu-03. The field-measured G_o values and the estimated ones are comparable or closely aligned. In the experimental field of EPUSP, resonant column tests with a Hardin oscillator were conducted on soil specimens to determine the

small-strain shear modulus, G_{max}, for various values of confining pressure. The moduli ranged from 130 MPa (for σ_3 equal to 100 kPa) to 220 MPa (for σ_3 equal to 300 kPa). In concordance with Figure 6, the values of G_o are close to those studied herein.

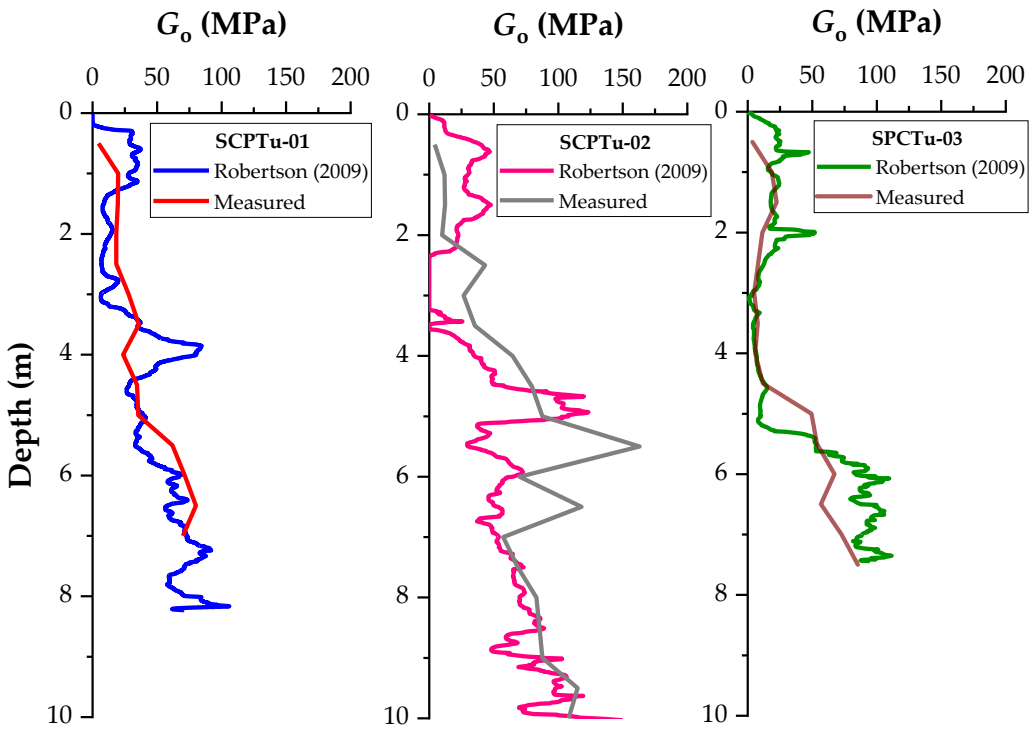

Figure 6. Comparison between G_o measured with accelerometers and G_o estimated with [35] for SCPTu-01, SCPTu-02, and SCPTu-03.

Taking as a guideline the boundaries defined by Schnaid et al. [8], theoretical results of q_c and G_o for sands and clays were produced based on formulations developed from calibration chamber tests. Formulations were selected that allowed the determination of these parameters based on the intrinsic properties of these materials, such as friction angle and relative density for sands and OCR for clays. Thus, by varying the values of these properties, it was possible to identify changes within the G_o/q_c versus Q_{tn} space, attributing a behavioral trend similar to the analysis performed from laboratory tests, as presented in Figure 7. While evaluating the test results from different types of deposits, it was observed that between the regions defined for sandy and clayey soils there exists a transitional region corresponding to intermediate silty soils, following a smooth transition and with the same trend as the boundary lines. Thus, it was found that the slope of the boundary lines is a combination of void ratio, mean stress, and soil critical state parameters and is not influenced by the soil type. Vertical lines were introduced to delineate transitions between different materials, which, like the lower boundary line for clays, are empirical, established from field test results, and are used to complement the classification system [4].

It is also noted in Figure 7 that a large percentage of the estimated shear modulus data fits satisfactorily within the limits established in the proposal by Schnaid et al. [8], supporting the previously shown soil classification result, which considers the soil in the studied area as freshly deposited, without aging or cementation. It is observed that a small percentage of the data falls below the lower limit of uncemented sandy soils, likely due to soils located near the surface, thus representing more recent depositions.

In the proposed classification system (Figure 7), the natural cementation process can be adequately identified as it induces an increase in the maximum shear modulus of the soil (G_o), although the strength remains relatively constant. On the other hand, the aging process tends to increase both the stiffness and strength due to particle interlocking.

Consequently, data points for cemented and aging sands are situated in the upper part of the region defined for uncemented sands. This situation justifies a higher value for the coefficient q_{c1}, which defines the upper boundary for cemented soils. A similar behavior was also observed in the analysis of laboratory test results for cemented materials studied by Schnaid [8] and Odebrech et al. [4].

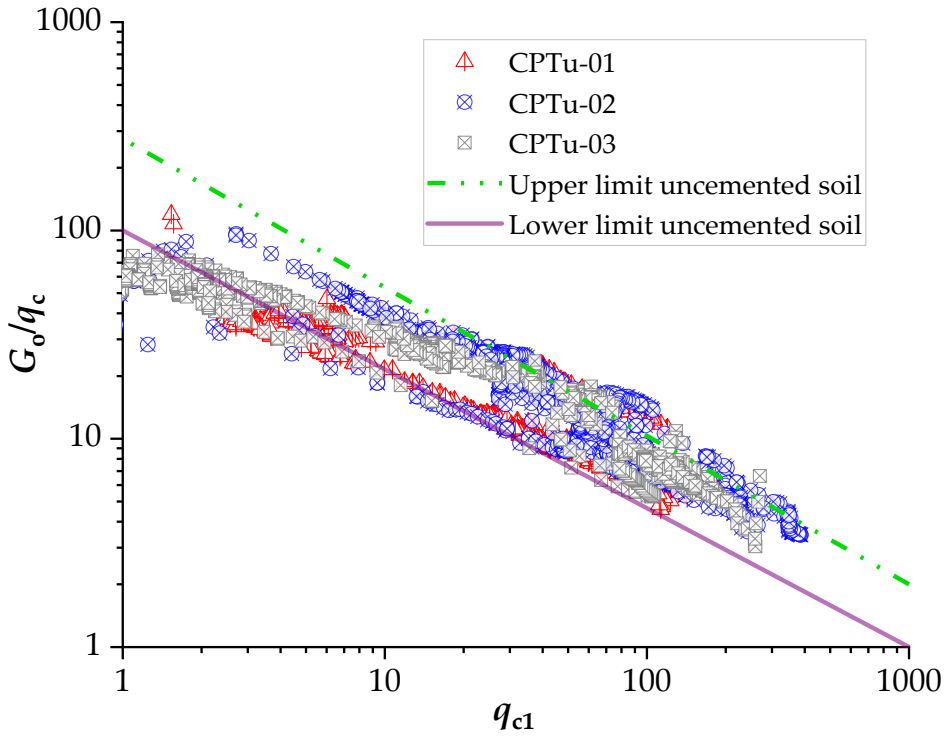

Figure 7. Normalized Maximum shear modulus and limits of uncemented soils.

Evaluating the test results from different types of deposits, it was observed that a transitional region corresponding to intermediate silty soils exists between the regions defined for sandy and clayey soils. This transition occurs smoothly and follows the same trend as the boundary lines. Thus, it was noted that the slope of the boundary lines is a combination of the soil's void ratio, mean stress, and critical state parameters, seemingly unaffected by the soil type. Vertical transition lines were introduced to delineate transitions between distinct materials. Similar to the lower limit line for clays, these lines are empirical, established based on field test results, and are used to complement the classification system.

Figure 8 presents the proof of the dissipation of pore pressure during CPTu testing. The depths and dissipation times are presented in detail in Table 1. As presented in the results, the excess water pressure was not recorded as more than 100 kPa, but in CPTu-03 at 5.24 m, it was identified as clay soil (Figure 5), and a pore pressure of 380 kPa was measured. Dissipation testing demonstrates that soils over 5 m have a sand behavior in concordance with the soil classification in Figure 5.

Figure 9 presents the soil's mechanical properties and unit weight estimation for the three points where the piezocone tests were conducted. Additionally, the variation of the I_c index is presented. These properties were estimating the equations proposed by Robertson [36] and Robertson and Cabal [37]. Soil total unit weights (γ) are best obtained by taking relatively undisturbed samples (e.g., thin-walled Shelby tubes; piston samples) and weighing a known volume of soil. When this is not feasible (as a present study), the total unit weight can be estimated from CPT results in concordance with Equation (4):

$$\gamma/\gamma_w = 0.27\ [\log\ \mathrm{Fr}] + 0.36\ [\log(q_t/p_a] + 1.236 \quad (4)$$

where γ_w is the unit weight of water. The friction angle ϕ' is estimated as (Equation (5)):

$$\phi\prime = 0.37\,[\log(q_c/\sigma'_{vo}) + 0.29] \quad (5)$$

Theoretical solutions have provided valuable insight into the relationship between cone resistance and undrained strength s_u. All theories result in a relationship between cone resistance and s_u of the form (Equation (6)):

$$S_u = (q_t - \sigma_{vo})/N_{kt} \quad (6)$$

N_{kt} is a preliminary cone factor value; typically, N_{kt} varies from 10 to 18. To simplify the application of the CPTu SBT chart shown in Figure 5, the normalized cone parameters Q_{tn} and Fr can be combined into one Soil Behavior Type index, I_c, where I_c is the radius of the essentially concentric circles that represent the boundaries between each SBT zone. I_c can be defined as follows (Equation (7)):

$$I_c = ((3.47 - \log Q_{tn})^2 + (\log \mathrm{Fr} + 1.22)^2)^{0.5} \quad (7)$$

The friction angle at the three points where the tests were conducted varied from 30 to 45 degrees, with average values of 40 degrees, typical of sandy soils. Small lenses of soils with a significant percentage of fines cross the granular layers, which can be attributed to the low estimated values for this parameter.

On the other hand, undrained strength was found in some soil intervals where compressible clays varied up to 200 kPa. The unit weights ranged from 14 to 19 kN/m^3. The specific weight results are consistent across the various borehole profiles, with values falling within the typical range for granular soils. The decrease in specific weight values observed at a depth of 3 m is likely determined by the significant amount of fines mixed with the sand. Finally, the I_c index demonstrates that the soil behavior is predominantly sandy, with values greater than 1.5.

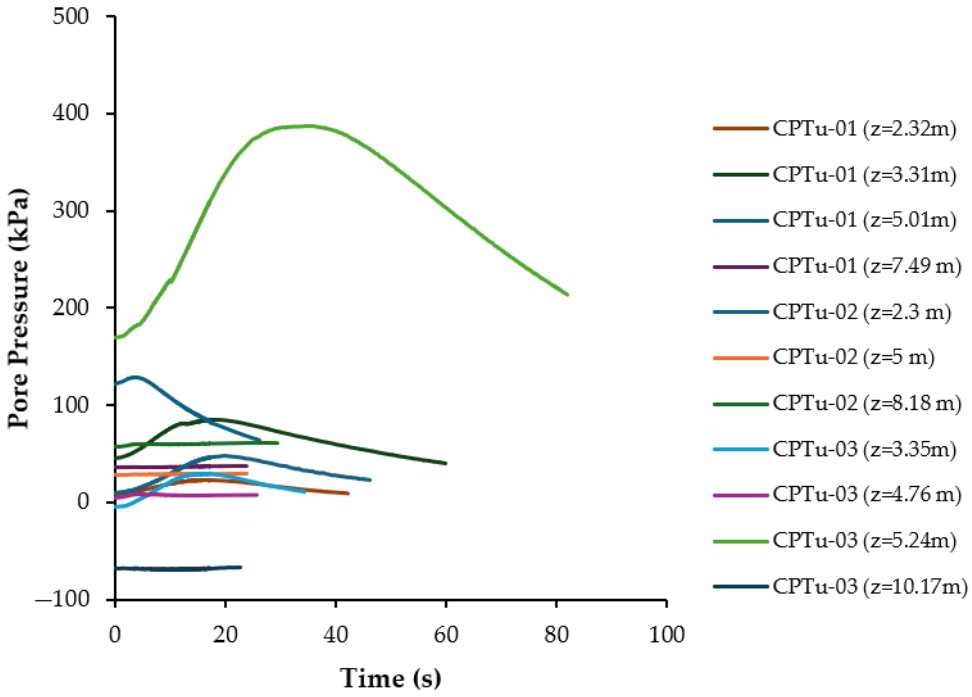

Figure 8. Dissipation time curing CPTu testing.

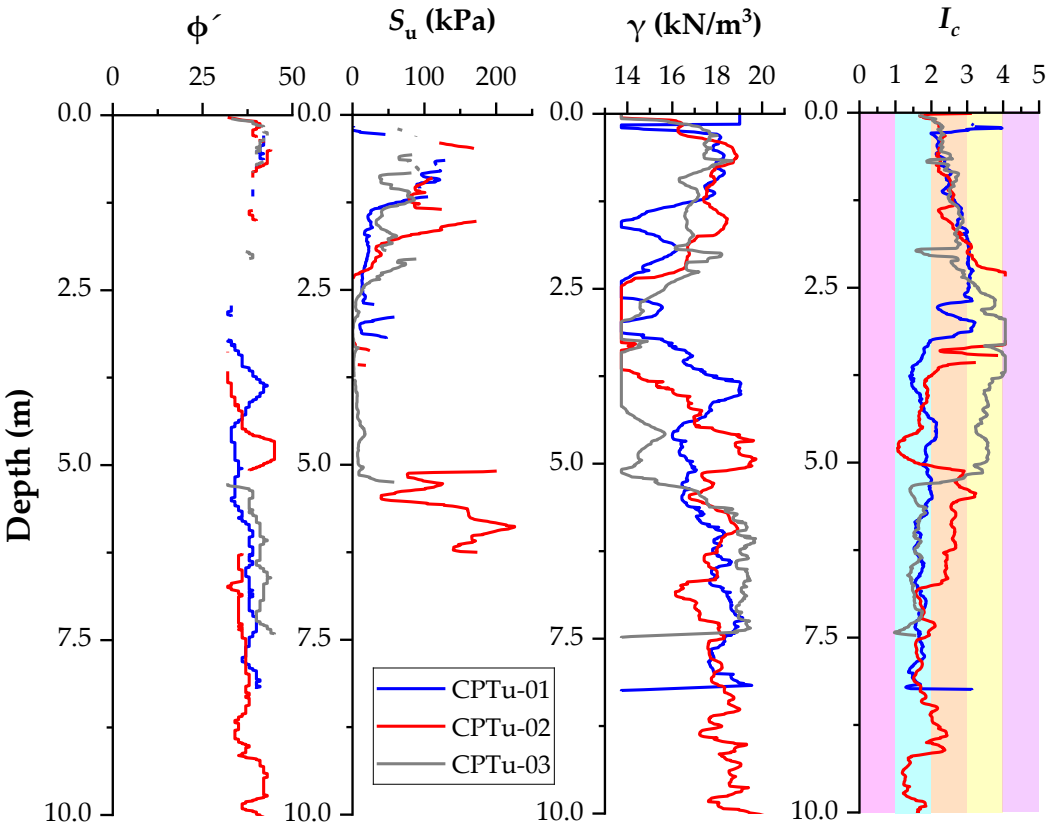

Figure 9. Estimation of internal friction angle (ϕ′), undrained strength (S_u), unit weight (γ), and I_c index.

3.2. Assessment of State Properties and Susceptibility to Liquefaction

Liquefaction flow is responsible for catastrophic damage triggered by sudden ruptures, spreading the liquefied material over large areas. In this context, based on the previously proposed classification system, an analysis was carried out to evaluate the flow potential due to the liquefaction of soil based on concepts from the critical state theory.

According to Schnaid and Yu [34] and Schnaid et al. [38], the value of state parameter ψ in sands can be obtained from a theoretical equation dependent on the G_o/q_t ratio. It is intended to investigate the applicability of this equation also for use in mining tailings (non-plastic silts). Considering the results of cone tests and tests with seismic readings, Schnaid and Yu [34] presented a theoretical correlation calibrated through tests conducted in a calibration chamber for determining the state parameter of clean sands, as presented by Equation (8).

$$\psi = \alpha \left(\frac{p'}{p_a} \right)^{\beta} + \chi \ln \left(\frac{G_o}{q_c} \right) \quad (8)$$

where $\alpha = -0.520$, $\beta = -0.07$, and $\chi = 0.180$ are average coefficients obtained from the data of tests in the calibration chamber, and p' is the average effective stress acting on the material. Whenever the material is in a dense state, with a void content initial value lower than the void ratio in the critical state, the material will have a dilatant behavior during shear, and ψ will assume a negative value. On the other hand, when the soil is in a soft state, with an initial void ratio higher than the critical void ratio, the soil will compress during shear, and ψ will assume a positive value. The conditions necessary for liquefaction flow in materials from the leftmost regions of the classification graph are different from those for materials located further to the right of the graph. In this way, knowing that both the soil classification system and the determination of the state parameter depend on the values of stiffness (G_o) and resistance (q_t), an equation was developed for delimiting

curves, with values defined from G_o, for which the state parameter is equal to zero. These curves were plotted with the classification system, as shown in Figure 10. The development of the soil classification system is based on theoretical formulations grounded in cavity expansion theory and critical state theory. This system allows for behavior analysis by combining stiffness and resistance parameters. In the case of application to sandy soils of the experimental field studied herein, the significant advantage of the system is linked to the identification of partial drainage conditions and the determination of a region for non-plastic sensitive materials, in which the generation of excess pore pressures occurs during cone penetration, with a significant reduction in tip resistance.

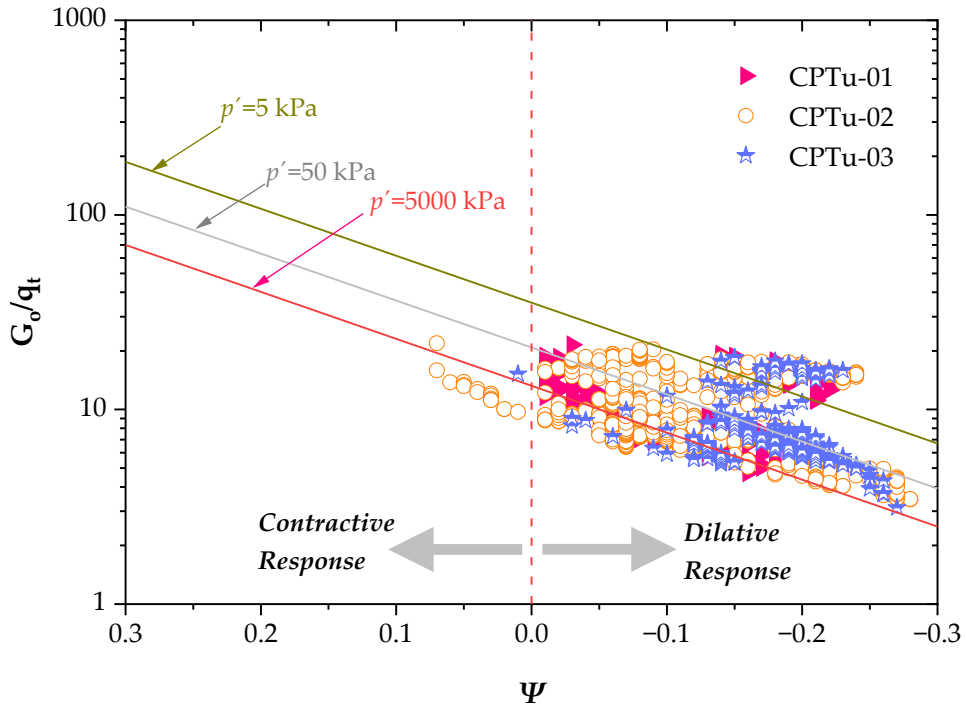

Figure 10. The methodology outlined by Schnaid et al. [38] for the classification and assessment of the state parameter value of sands using CPTu tests, compared with CPTu-01, CPTu-02, and CPTu-03.

Thus, Figure 10 presents the relationship between G_o/q_t for the CPTu results, whose outcomes were compared to values in the calibration chamber for a stress range between 50 and 5000 kPa. It is observed that for a certain stress level, the ratio of G_o/q_t decreases with the reduction of the state parameter value ψ; that is, G_o/q_t decreases with the increase in the relative density of the material. As presented in Figure 10, the data recorded on the CPTu tests demonstrates that soils are classified as dilative material. In this context, the material is susceptible to liquefaction, as explained by Schnaid et al. [35,38].

Keeping the G_o value fixed, the state parameter decreases to the right of the presented curve and increases to the left. From Figures 7 and 10 of the curves of different values of G_o with null state parameter, it can be inferred that, for example, for a material with G_o = 100,000 kPa to have susceptibility to the occurrence of liquefaction flow ($\psi > 0$) the same must present values of q_t such that they produce a combination of G_o/q_t and Q_{tn} positioned to the left of the line defined for G_o = 100,000 and null state parameter. The analysis is the same for the case of G_o's different values. As verified in the classification methodology, there is a specific dispersion in the data, a fact justified by soil anisotropy, stress history, presence of fines, and drainage conditions. Despite this condition, the results from the database are within pre-established limits and follow the behavior information presented in the literature. Moreover, the values greater than 0, indicating a contractive response in non-plastic soils, are susceptible to liquefaction flow occurrence, as reported by [4,8,17,38].

3.3. Standard Penetration Test SPT and SPT-Torque

The groundwater level was determined at the end of the test using a probe inserted into the borehole to locate it. The groundwater level was found to be at 2.0 m in this manner. Dissipation tests were also conducted in the piezocone (Table 1) to verify these results. The number of blows corresponding to 72% efficiency was considered.

Figure 11 presents the results of SPT-Torque tests on the soil profile. In the first 5 m of soil, fine soils such as silty clays and clayey silts can be found. In the initial meters of the SPT-1 region, clay fills can be found, which were caused by earth movements of anthropogenic origin during the construction of nearby buildings. The presence of the channel causes part of this artificial fill to degrade during flood seasons. N_{SPT} values varied from 2 to 10 during the first 5 m. From 5 to 25 m, N_{SPT} values of 20 blows on average were found, corresponding to more representative values for fine to medium sands. A visual inspection has been carried out to confirm the soil classification. For the torque values, Figure 11 presents, for each test, the measured force to rotate the SPT sampler. Torque values have been measured up to 15 m, ranging from 0 to 8 kgf·m in the first 7 m, reaching average measurements of 20 kgf·m, confirming the presence of sandy material up to 25 m deep. Residual torque values ranged from 5 to 15 kgf·m. The representative curves of inceptisols showed a maximum torque of 60° before rotation. The residual torque was well-defined before the second complete turn. Additionally, the histosols of São Paulo reached the torque maximum almost instantly. The residual torque dropped rapidly, and after the third turn, the value increased slightly, making it difficult to set a correct value.

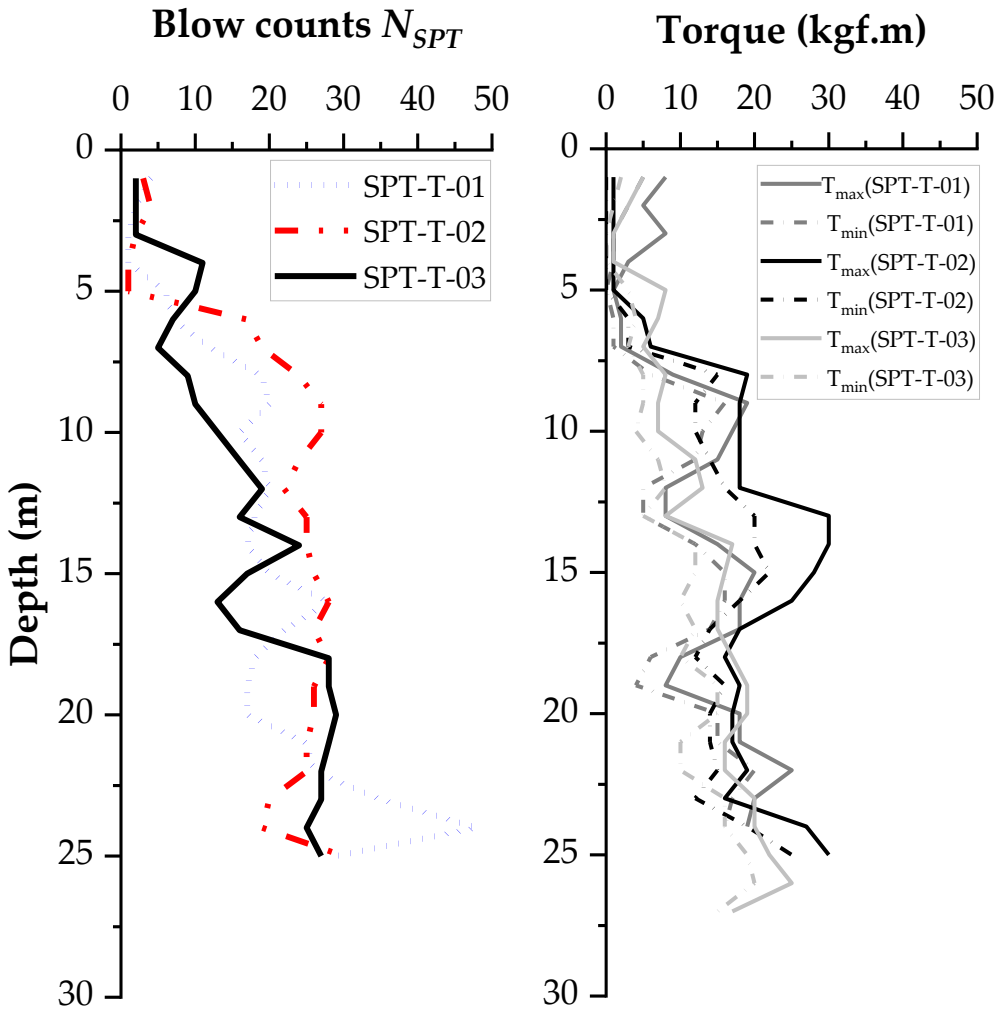

Figure 11. Soil profile with SPT-T values: blow counts and torque.

3.4. Soil Profile

Based on the data from CPTu and SPT-T, the geotechnical profile of the experimental field was created. Figure 12 shows the soil profile along the measured area. Clayey and loamy soils can be found up to the first 2.5 m, and from 2.5 m to 5.8 m, medium sands with clays were encountered. From 6 m to 25 m, a homogeneous profile of dense and medium sands can be found, except near the SPT-1 region, where stiff clay was encountered at the end of the borehole. According to Figure 4, the three CPTu boreholes generally show good correspondence. The distinction between the profiles is limited to the variability in the resistance of the sand layer in the first horizon and the position of the clay layer. In this regard, it was possible to tentatively delineate the three horizons shown in Figure 12 up to 8 m, in correspondence to CPTu data and SPT. From a depth of 8 m, where cone tests were not conducted, the soil horizons were classified solely using the SPT. These horizons mostly correspond to sands, with some areas containing cohesive soils. These horizons result from the approximation of the behavior of the analyzed soils.

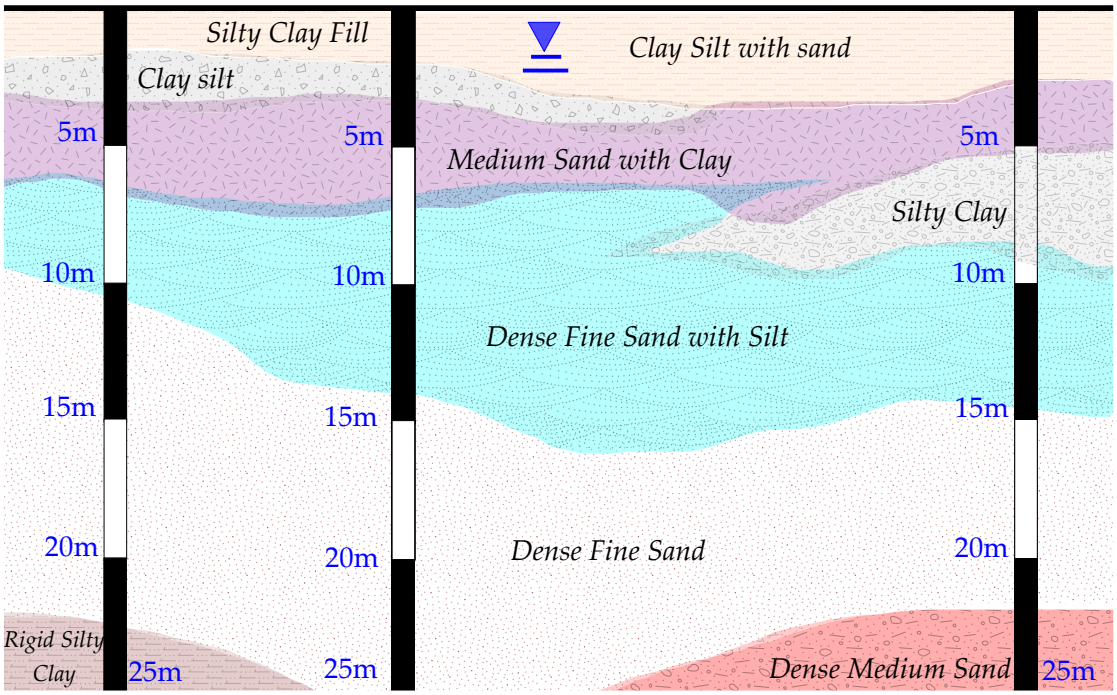

Figure 12. Soil Classification Profile of Experimental Site based on SPT-T and CPTu tests.

3.5. Soil Classification of Characteristic Sand Sample

The sandy soil sample was extracted during SPT testing. The depth collected was 3 m. The sand is composed of 30% medium sand by weight under Brazilian standard NBR 6502 [39]. The coefficient of curvature and uniformity were measured as 2.49 and 15.83, respectively, the effective diameter D_{10} = 0.008 mm, and the mean particle diameter (D_{50}) was calculated as 0.10 mm. The specific gravity of sand particles was measured as 2.72. The soil is classified as well-graded sand (SW) in agreement with the Unified Soil Classification System [40]. Scanning electron microscopy (SEM), Energy Dispersive X-ray (EDX) spectrometry, and X-ray fluorescence spectroscopy (FRX) with element detection were carried out on the sand samples. Figures 13 and 14 show the SEM and SEM-EDX positions and elements detection results.

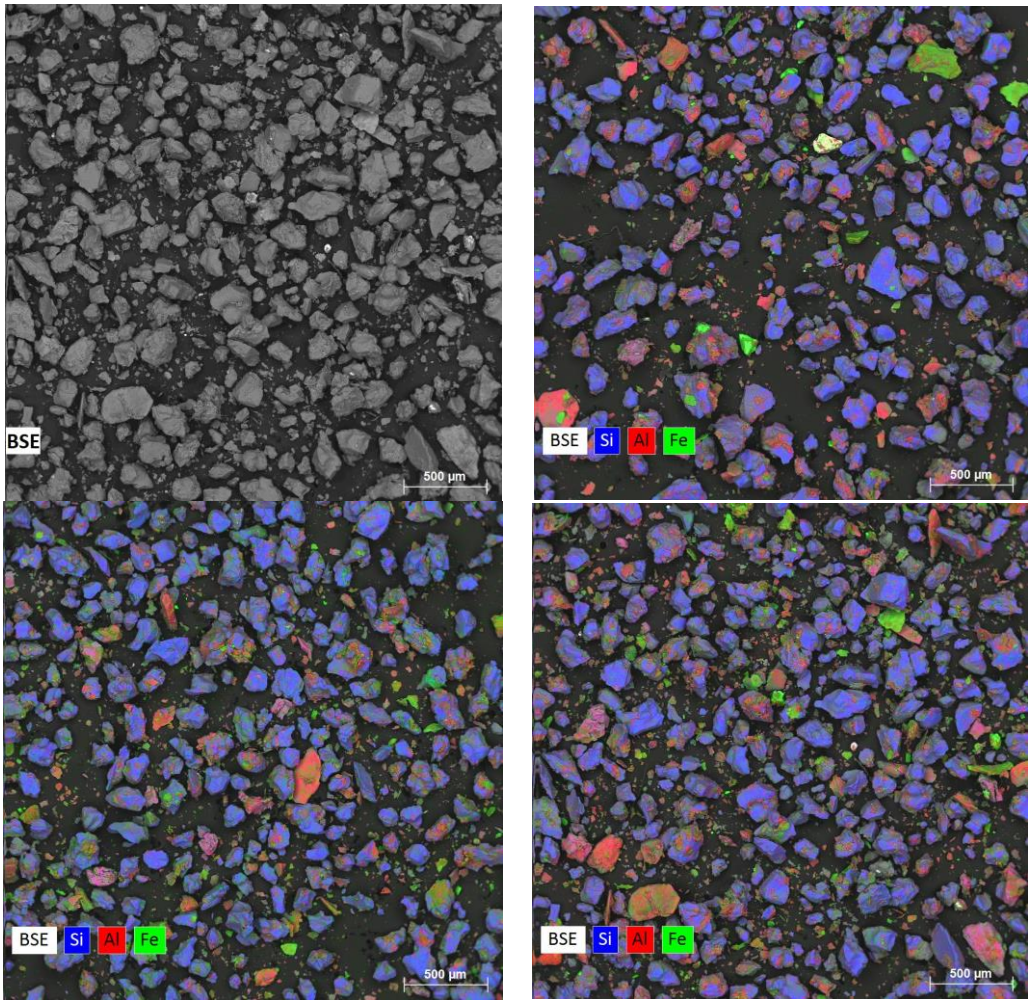

Figure 13. SEM micrographs of the sand sample collected.

The sandy soil contained quartz and mica minerals that were in concordance with XRD analysis. As shown in Figure 13, the sand particles are not uniform and have angularity. Backscattered-electron scanning electron microscopy (BSE-SEM) shows the detection of silicon, aluminum, and iron. BSE-SEM imaging is a valuable technique for materials characterization because it provides information about the homogeneity of the material in the analyzed sand specimens and is, therefore, an essential technique in modern SEM. Besides, XFR analysis detected 89.5% silicon, 5.42% aluminum, 1.23% iron, and other minor elements (i.e., K and Mg) by weight. Figure 14 presents the SEM-EDX analysis of the sand sample. Within the five analyzed positions, it can be analyzed that the soil presents the same chemical composition as that detected by the BSE-SEM and XRD.

When evaluating the behavior of a granular material under an external load, the active contacts between the grains will support these loads. Defining the active contacts supporting this load becomes more complicated when fine particles are present among larger particles. Thevanayagam et al. [41] identified three microstructural conditions for analyzing the behavior of granular materials with fines. In the first situation, the larger particles prevail over the smaller ones, which, depending on their quantity, can fill the spaces between the larger particles without contributing to the support of external loads. They may partially support the load or even separate the coarse particles. In the second condition, the fine particles are so high that they can separate the larger particles. Finally, in the last condition, the two types of soils form separate layers.

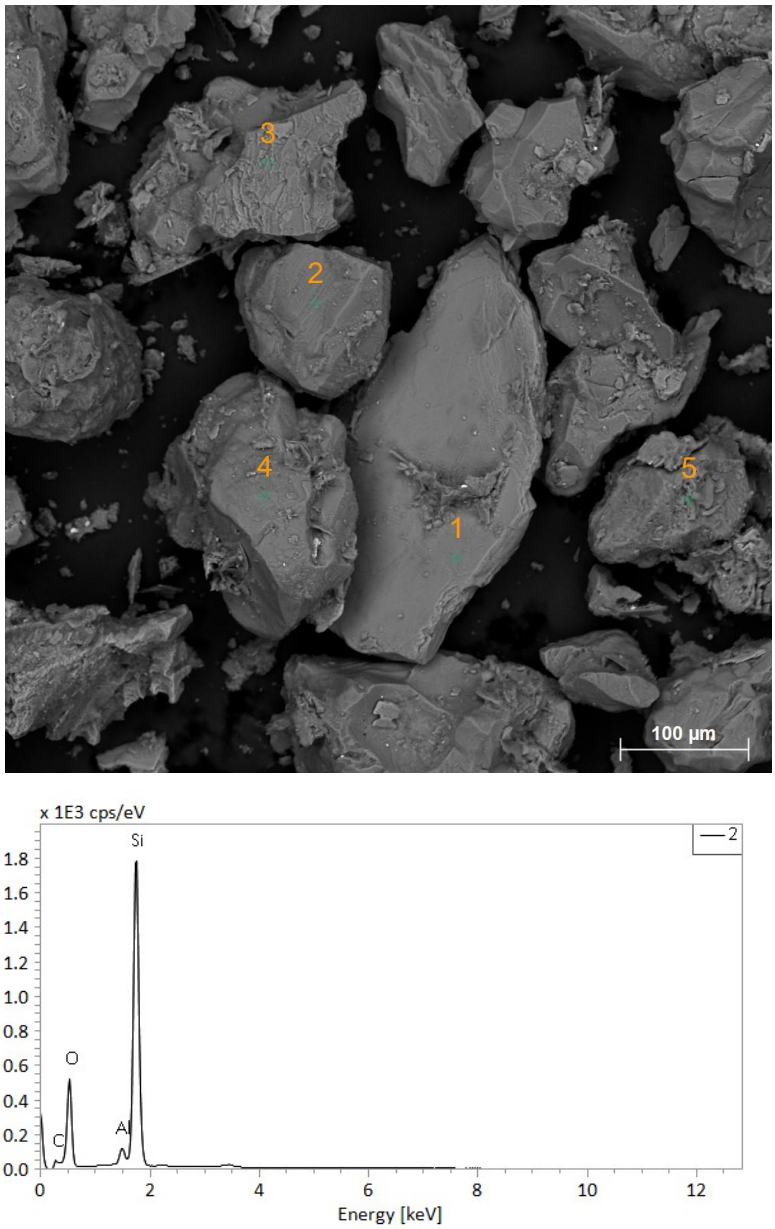

Figure 14. SEM micrographs of the sand sample were collected using EDX analysis.

3.6. Practical Applications and Future Research

This study presents a geomechanical and geotechnical analysis of an experimental field typical to São Paulo, Brazil. Recent studies demonstrate the use of this field, such as for characterization, monitoring, and modeling of pedestrian bridges [25,26]. Additionally, the analysis and design of deep foundations for building projects with energy and heat exchanger piles are demonstrated in recent studies within the experimental field [28]. Furthermore, for future research, we intend to use and implement the Thermal Cone Test (TCT) within the area, utilizing the same equipment from the Cone Penetration Test (CPTu). For this purpose, the cone must be equipped with a temperature sensor, and the test must be paused at depths of interest so that the excess heat generated during penetration can dissipate and time and temperature data can be recorded for subsequent interpretation. In the case of soft soils or shallow depths, it may be necessary to heat the cone to generate sufficient heat for the dissipation test.

This study performed a comprehensive geomechanical and geotechnical analysis of a typical São Paulo, Brazil profile. This research demonstrates the utility of the experimental

field for various applications, including the characterization and monitoring of pedestrian bridges and the design of deep foundations. Although widely used, existing analysis methods have notable limitations, such as the Standard Penetration Test (SPT), piezocone test (CPTu), and seismic CPTu. The SPT, while helpful in providing soil resistance data, can be highly variable and influenced by operator technique and equipment inconsistencies. Moreover, it offers limited information about soil stratigraphy and material properties. The CPTu test provides more detailed resistance variations and stratigraphic transitions but can be less effective in soils with significant heterogeneity or cementation. Additionally, seismic CPTu measurements, although beneficial for determining wave velocities and stiffness, may be constrained by equipment sensitivity and site-specific conditions.

By addressing these limitations through our integrated approach, which combines multiple testing methods and real-world field parameters, this study contributes to a more accurate and reliable characterization of subsurface conditions. Our findings underscore the need for advanced methodologies and calibrated models to enhance safety and stability analysis of deep foundations. The findings of this study have significant practical implications for architectural practice, foundation design, and geological risk assessment. In terms of architectural practice, the detailed geotechnical and geomechanical characterization of the experimental site provides architects with critical data for designing structures better adapted to local soil conditions. Understanding the soil's behavior under different loading conditions ensures that architectural designs are safe and sustainable. Integrating various testing methods yields comprehensive soil profiles for foundation design, allowing engineers to design foundations optimized for both performance and cost. The reliability of the CPTu and S-CPTu tests in identifying soil stratigraphy and mechanical properties supports the development of foundation solutions that can withstand local geotechnical challenges, thereby reducing the risk of settlement and other foundation-related issues. Furthermore, the study's findings enhance the ability to assess geological risks, such as soil liquefaction, slope instability, and seismic activity. By providing accurate soil behavior data, the research helps predict and mitigate the potential impacts of these risks on built structures. This is particularly crucial for ensuring the safety and resilience of infrastructure in regions prone to geological hazards.

The method proposed in this study is developed for the experimental field of the University of São Paulo and implemented in a particular geographical context. While the method demonstrates efficacy in the specific location where it was tested, its applicability to other locations warrants consideration. The soil characteristics, geological formations, and environmental conditions can vary significantly between different regions, potentially influencing the method's performance. Therefore, before extending the use of this method to other locations, further validation and adaptation may be necessary to ensure its suitability and reliability across diverse settings.

4. Conclusions

- The average profile of the area was determined from CPTu, SPT-T, and seismic tests. These tests provide similar results in terms of resistance variation with depth. However, the CPTu test offers more detailed information on resistance variations and the transition of profile properties.
- The materials identified in the profile of the studied area, ordered from greatest to least presence in the deposit, were interpreted as sandy soils; sandy silts; silty sands; silty clays; clayey silts; sand with gravel; and, to a lesser extent, clay soils.
- Through the piezocone test, it is possible to determine the classification of the soil stratigraphic profile based on its mechanical behavior characteristics on-site, including strength, stiffness, and the pore pressures induced by penetration. When comparing this stratigraphic profile with one obtained through soil sampling and laboratory tests, the conventional method for soil classification has demonstrated that it is a reasonably accurate approximation.

- The soils composing the studied deposit contain varying percentages of silty material. However, these soils exhibit rapid pore pressure dissipation, making it possible, in most of the profile, to estimate parameters that characterize them using typical correlations for sandy soils.
- Based on the geological studies consulted in the area of influence and the results of field and laboratory tests analyzed in this research, it can be inferred that the deposit in the study area is composed of non-cemented material.
- The soil comprising the studied deposit exhibits varying percentages of clayey material in the first 4 m and sandy material up to 25 m. However, these soils experience rapid pore pressure dissipation, allowing for the estimation of characteristic parameters through typical correlations for sandy soils for most of the profile.
- According to the G_o stiffness tests (seismic CPTu) conducted in the field, the initial calculations of the design parameters indicate that the studied deposit shows greater stiffness in the section from 5 to 11 m than in the shallower layers, with friction angles between 35 and 40 degrees.

Author Contributions: Conceptualization, J.d.J.A.B. and M.M.F.; methodology, J.d.J.A.B. and M.M.F.; software, J.d.J.A.B.; validation, Y.E.N.d.l.R. and M.M.F.; formal analysis, J.d.J.A.B.; investigation, J.d.J.A.B.; resources, M.M.F. and Y.E.N.d.l.R.; data curation, J.d.J.A.B.; writing—original draft preparation, J.d.J.A.B.; writing—review and editing, M.M.F. and Y.E.N.d.l.R.; visualization, J.d.J.A.B.; supervision, M.M.F.; project administration, M.M.F.; funding acquisition, M.M.F. and Y.E.N.d.l.R. All authors have read and agreed to the published version of the manuscript.

Funding: VALE Catedra under Rail Project and The Fundación Universitaria Los Libertadores—Colombia (FULL) (Project N° ING-39-24) funded the APC.

Institutional Review Board Statement: Not applicable.

Informed Consent Statement: Not applicable.

Data Availability Statement: Data are contained within the article.

Acknowledgments: The authors thank the VALE Catedra Under Rail for providing financial support to develop this research, and Damasco Penna-Engenharia Geotecnica for carrying out the geotechnical site investigation.

Conflicts of Interest: The authors declare no conflicts of interest.

References

1. Cavalcante, E.; Danziger, F.; Giacheti, H.; Coutinho, R.; Souza, A. Campos Experimentais Brasileiros. *Geotecnia* **2007**, 99–205. [CrossRef]
2. Khan, Z.; Yamin, M.; Attom, M.; Al Hai, N. Correlations between SPT, CPT, and Vs for Reclaimed Lands near Dubai. *Geotech. Geol. Eng.* **2022**, *40*, 4109–4120. [CrossRef]
3. Zhou, J.; Li, E.; Wang, M.; Chen, X.; Shi, X.; Jiang, L. Feasibility of Stochastic Gradient Boosting Approach for Evaluating Seismic Liquefaction Potential Based on SPT and CPT Case Histories. *J. Perform. Constr. Facil.* **2019**, *33*, 04019024. [CrossRef]
4. Odebrecht, E.; Mantaras, F.M.B.; Schnaid, F. A Method for Predicting the Undrained Shear Strength from Piezocone Dissipation Test. In Proceedings of the Cone Penetration Testing 2018—4th International Symposium on Cone Penetration Testing, CPT 2018, Delft, The Netherlands, 21–22 June 2018.
5. Robertson, P.K. Soil Behaviour Type from the CPT: An Update. In Proceedings of the 2nd International Symposium on Cone Penetration Testing, Hundtington Beach, CA, USA, 9–11 May 2010.
6. Robertson, P.K.; Fear, C.E.; Woeller, D.J.; Weemees, I. Estimation of Sand Compressibility from Seismic CPT. In Proceedings of the 48th Canadian Geotechnical Conference, Vancouver, BC, Canada, 25–27 September 1995.
7. Eslaamizaad, S.; Robertson, P.K. Evaluation of Settlement of Footings on Sand from Seismic In-Sity Tests. In Proceedings of the 50th Canadian Geotechnical Conference, Ottawa, ON, Canada, 20–22 October 1997; pp. 20–22.
8. Schnaid, F. Geo-Characterisation and Properties of Natural Soils by in Situ Tests. In Proceedings of the 16th International Conference on Soil Mechanics and Geotechnical Engineering: Geotechnology in Harmony with the Global Environment, Osaka, Japan, 12–16 September 2005; Volume 1.
9. Collico, S.; Arroyo, M. Bayesian Mixture Analysis of a Global Database to Improve Unit Weight Prediction from CPTu. *Eng. Geol.* **2023**, *327*, 107353. [CrossRef]

10. Collico, S.; Arroyo, M.; Kopf, A.; Devincenzi, M. A Probabilistic Bayesian Methodology for the Strain-Rate Correction of Dynamic CPTu Data. *Can. Geotech. J.* **2023**, *60*, 669–686. [CrossRef]
11. Collico, S.; Arroyo, M.; Devincenzi, M. A Simple Approach to Probabilistic CPTu-Based Geotechnical Stratigraphic Profiling. *Comput. Geotech.* **2024**, *165*, 105905. [CrossRef]
12. Boschi, K.; Arroyo, M.; Monforte, L.; Carbonell, J.M.; Gens, A. Coupled Hydromechanical Modelling of Cone Penetration in Layered Liquefiable Soils. *Géotechnique* **2024**, 1–15. [CrossRef]
13. Zhang, M.; Tong, L. Statistical Assessment of Simplified CPTU-Based Hydraulic Conductivity Curves. *Geofluids* **2021**, *2021*, 6656867. [CrossRef]
14. Młynarek, Z.; Wierzbicki, J.; Lunne, T. Usefulness of the CPTU Method in Evaluating Shear Modulus G0changes in the Subsoil. *Stud. Geotech. Mech.* **2021**, *43*, 195–205. [CrossRef]
15. Liu, X.; Congress, S.S.C.; Cai, G.; Liu, L.; Liu, S.; Puppala, A.J.; Zhang, W. Development and Validation of a Method to Predict the Soil Thermal Conductivity Using Thermal Piezocone Penetration Testing (T-CPTU). *Can. Geotech. J.* **2022**, *59*, 510–525. [CrossRef]
16. Zhang, M.; Tong, L.; Wang, Q. Geotechnical Characteristic Assessments of Floodplain Soils Using SCPTU Data in Nanjing, China. *Adv. Civ. Eng.* **2022**, *2022*, 1669511. [CrossRef]
17. Monforte, L.; Arroyo, M.; Gens, A. A Relation between Undrained CPTu Results and the State Parameter for Liquefiable Soils. *Can. Geotech. J.* **2023**, *60*, 1756–1774. [CrossRef]
18. Nandi, S.; Bandyopadhyay, K.; Basu, D.; Shiuly, A. Correlation of Pressuremeter Test Results with SPT N Values and Liquidity Index for Cohesive Soil of Normal Calcutta Deposit. *Indian Geotech. J.* **2024**. [CrossRef]
19. San Roman Iturbide, O.; Botero Jaramillo, E. Identification of Geotechnical Units in Soil Exploration through Principal Component Analysis and Clustering. *Int. J. Numer. Anal. Methods Geomech.* **2024**, *48*, 1681–1699. [CrossRef]
20. Sharma, A.; Samanta, M.; Kanungo, D.P. Site-Specific Correlation between Geotechnical and Geoelectrical Properties of Soil Deposits in India. *J. Appl. Geophy.* **2024**, *221*, 105288. [CrossRef]
21. Puttiwongrak, A.; Keo, S.; Vann, S.; Arpornthip, T.; Suteerasak, T.; Sukontasukkul, P. Geological and Climatic Factors Affecting the Correlation between Electrical Resistivity and SPT N-Value in Sandy Soils of Phuket, Thailand. *Geosciences* **2023**, *13*, 185. [CrossRef]
22. Hegde, A.; Anand, A. Resistivity Correlations with SPT-N and Shear Wave Velocity for Patna Soil in India. *Indian Geotech. J.* **2022**, *52*, 161–173. [CrossRef]
23. Bol, E. A New Approach to the Correlation of SPT-CPT Depending on the Soil Behavior Type Index. *Eng. Geol.* **2023**, *314*, 106996. [CrossRef]
24. Rocha, B.P.; da Silva, B.C.; Giacheti, H.L. Maximum Shear Modulus Estimative from SPT for Some Brazilian Tropical Soils. *Soils Rocks* **2023**, *46*, e2023005222. [CrossRef]
25. Gamino, A.L.; Hune, R.P.; Santos, R.R.; de Bragança, C.S.C.; Bittencourt, T.N.; Carvalho, H.; Futai, M.M. Dynamic Analysis of a Pedestrian Bridge Using Monitoring and Computational Techniques. *Preprints* **2023**. [CrossRef]
26. Gamino, A.L.; do Amaral, M.A.; Santos, R.R.; Menezes, G.V.; Bittencourt, T.N.; Futai, M.M. Soil-Structure Interaction Approach of a Timber-Concrete Composite Pedestrian Bridge. *Pract. Period. Struct. Des. Constr.* **2023**, *28*, 04023018. [CrossRef]
27. Cardoso de Freitas Murari, M.; de Hollanda Cavalcanti Tsuha, C.; Loveridge, F. Investigation on the Thermal Response of Steel Pipe Energy Piles with Different Backfill Materials. *Renew Energy* **2022**, *199*, 44–61. [CrossRef]
28. Pessin, J.; de Hollanda Cavalcanti Tsuha, C. In-Field Performance of Continuous Flight Auger (CFA) Energy Piles with Different Configurations. *Appl. Therm. Eng.* **2023**, *224*, 120113. [CrossRef]
29. *ASTM D6635-15*; Standard Test Method for Performing the Flat Plate Dilatometer. ASTM International: West Conshohocken, PA, USA, 2015.
30. British Standards Institution. Eurocode 7 Geotechnical Design. Part 1. In *Structural Engineer, (Together with United Kingdom National Application Document)*; British Standards Institution: London, UK, 2009; p. 87.
31. *ABNT ABNT NBR 6484*; Solo—Sondagem de Simples Reconhecimento Com SPT—Método de Ensaio. ABNT: Rio de Janeiro, Brazil, 2020.
32. *NBR NBR 6122*; Projeto e Execução de Fundações. Associação Brasileira de Normas Técnicas: Rio de Janeiro, Brazil, 2019.
33. Lunne, T.; Powell, J.J.M.; Robertson, P.K. *Cone Penetration Testing in Geotechnical Practice*; CRC Press: Boca Raton, FL, USA, 2002; ISBN 1482295040.
34. Schnaid, F.; Yu, H.S. Interpretation of the Seismic Cone Test in Granular Soils. *Geotechnique* **2007**, *57*, 265–272. [CrossRef]
35. Robertson, P.K. Interpretation of Cone Penetration Tests—A Unified Approach. *Can. Geotech. J.* **2009**, *46*, 1337–1355. [CrossRef]
36. Robertson, P.K. Cone Penetration Test (CPT)-Based Soil Behaviour Type (SBT) Classification System—An Update. *Can. Geotech. J.* **2016**, *53*, 1910–1927. [CrossRef]
37. Robertson, P.K.; Cabal, K.L. *Guide to Cone Penetration Testing for Geotechnical Engineering*; Gregg Drilling & Testing, Inc.: Benicia, CA, USA, 2010.
38. Schnaid, F.; Nierwinski, H.P.; Odebrecht, E. Classification and State-Parameter Assessment of Granular Soils Using the Seismic Cone. *J. Geotech. Geoenviron. Eng.* **2020**, *146*, 06020009. [CrossRef]
39. *ABNT NBR 6502*; Rochas e Solos. Associação Brasileira de Normas Técnicas: Rio de Janeiro, Brazil, 1995.

40. *ASTM ASTM D2487*; Standard Practice for Classification of Soils for Engineering Purposes (Unified Soil Classification System). ASTM International: West Conshohocken, PA, USA, 2011; pp. 1–16. [CrossRef]
41. Thevanayagam, S.; Shenthan, T.; Mohan, S.; Liang, J. Undrained Fragility of Clean Sands, Silty Sands, and Sandy Silts. *J. Geotech. Geoenviron. Eng.* **2002**, *128*, 849–859. [CrossRef]

Disclaimer/Publisher's Note: The statements, opinions and data contained in all publications are solely those of the individual author(s) and contributor(s) and not of MDPI and/or the editor(s). MDPI and/or the editor(s) disclaim responsibility for any injury to people or property resulting from any ideas, methods, instructions or products referred to in the content.